5G in Open-Pit Mines

Considerations on Large-Scale Propagation in Sub-6 GHz Bands

Portela Lopes de Almeida, Erika; Caldwell, George; Rodriguez Larrad, Ignacio; Vieira, Robson; Sørensen, Troels Bundgaard; Mogensen, Preben Elgaard; Garcia, Luis G. U.

Published in:
IEEE Globecom Workshops 2017

DOI (link to publication from Publisher):
10.1109/GLOCOMW.2017.8269056

Publication date:
2017

Document Version
Accepted author manuscript, peer reviewed version

5G in Open-Pit Mines: Considerations on Large-Scale Propagation in Sub-6 GHz Bands

Erika P. L. Almeida[1,2], George Caldwell[3], Ignacio Rodriguez[1], Robson D. Vieira[3], Troels B. Sørensen[1], Preben Mogensen[1] and Luis G. Uzeda Garcia[4]

[1]Department of Electronic Systems, Aalborg University (AAU), Denmark.
[2]Technology Development Institute (INDT), Brazil.
[3]Ektrum, Brazil. [4]Instituto Tecnológico Vale (ITV), Brazil.

***Abstract*—5G will play a pivotal role in the digitization of the industrial sector and is expected to make the best use of every bit of spectrum available. In this light, this paper presents the results of an extensive measurement campaign in two iron-ore open-pit mining complexes, at the 700 MHz and 2.6 GHz bands, considering macro and small cell deployments. The study is further motivated by the rise of unmanned machinery in the mining industry. We present values of path loss exponents, shadow fading standard deviations, autocorrelation distances and inter-frequency cross-correlation, which are all useful for the future wireless network design, simulation and performance evaluation. The results show that, in order to comply with ultra-reliable communications (URC) availability requirements, larger shadowing margins will have to be considered in the network planning in open-pit mines, when compared to traditional industrial environments. Furthermore, large cross-correlation between the shadowing in both frequency bands limits the gains when using multi-connectivity in order to enhance overall network availability.**

I. Introduction

The mining industry has a long history of reliance on wireless communications; radio was initially introduced to support mission-critical voice services. Gradually, new applications such as fleet management, real-time telemetry and GPS-augmentation systems required those voice networks to be complemented by narrowband solutions, such as TETRA and TEDS. Lately, broadband technologies such as WiMAX, Wi-Fi and even LTE coexist with narrowband technologies, supporting applications such as video surveillance, real-time data acquisition and analytics [1], [2].

The need for continuous safety improvements and increased operational efficiency is pushing this industry towards unmanned operations. In fact, large-scale automation initiatives are already a reality at mine sites around the world [3]. New applications such as autonomous haulage systems (AHS), teleoperated bulldozers and excavators pose much more strict requirements in terms of network availability, accessibility, reliability, capacity and latency when compared to previous applications [4], [5]. In practice, the industrial networking requirements set by robotic mining are in line with those associated with URC in 5G wireless systems [5]–[7].

However, due to the peculiar scenario and nature of operation, surface mining sites differ from traditional indoor industrial environments. For example, open-pit mines are outdoor scenarios, usually kilometers wide, and hundreds of meters deep. Furthermore, due to the nature of the mining activity, the scenario changes on a daily basis, also modifying the propagation environment [3].

In order to achieve such stringent availability requirements in a wireless network, it is crucial to have a deep understanding of the radio propagation channel. Despite the mining industry reliance on wireless communications, radio propagation in surface mines has not been explored as extensively as in underground mines [8]. In the case of open-pit mines, only a limited set of references was found. In [9], a geometric model is proposed based on the complete knowledge of the environment, however no measurements were presented to testify the results. In [10] the authors present a study of the channel impulse response in the 2.4 GHz band, based on wideband channel sounding. The conclusion is that the increased delay spread limits the performance of orthogonal division multiplexing (OFDM) systems such as LTE and Wi-Fi, with standard values of cyclic prefix. In a previous work [11], we proposed three path loss models based on measurements in the 2.6 GHz band and showed that, also from the radio propagation perspective, there are no two mines alike.

While there is no doubt that millimeter wave bands will be important for future 5G solutions in industrial scenarios, sub-6GHz spectrum is also very attractive in terms of cost and usability. Therefore, the aim of this paper is to present and discuss recent measurement results at low- and mid-bands, namely the 700 MHz (sub-1GHz) and the 2.6 GHz spectrum bands in open-pit mining scenarios. Here, we investigate large scale propagation in terms of path loss, shadowing, shadowing correlation distance and inter-frequency shadowing correlation. Those values are important to standardization forums and for evaluating future URC technology in this environment.

The remainder of this paper is organized as follows. Section II describes the measurement scenario, setup and the data processing. Section III presents the results and discusses their implications on the design of reliable networks in open-pit mines. Finally, Section IV concludes the paper.

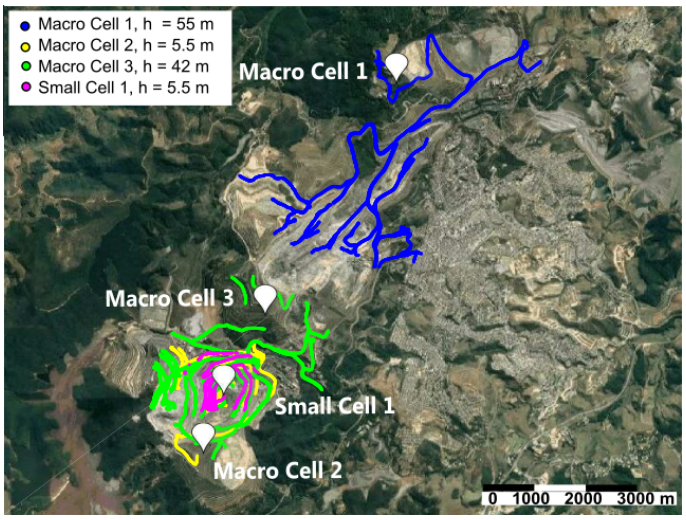

Figure 1. Measurement routes and transmitter positions in Mine 1. The height above ground level, h, is also displayed in the legend.

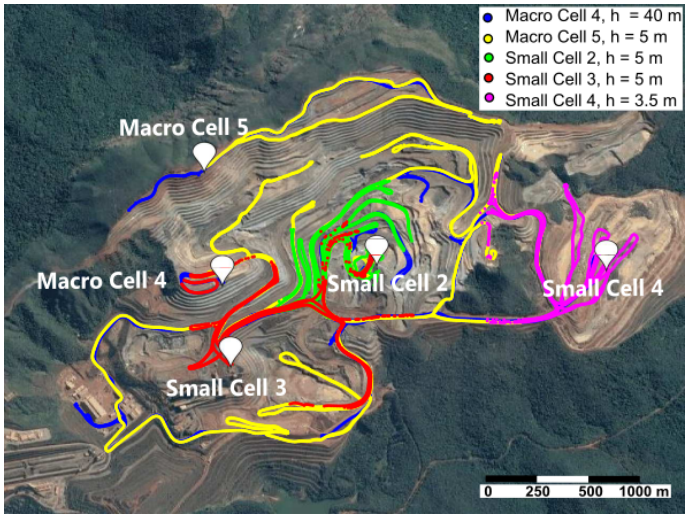

Figure 2. Measurement routes and transmitter positions in Mine 2. The height above ground level, h, is also displayed in the legend.

II. Methodology

In this section, we describe the methodology used in the measurement campaign and further data processing. The measurement campaign was performed in two iron-ore open-pit mine complexes located in Brazil, between April and May 2017. Figures 1 and 2 show aerial views of these mines, as well as the measurement routes and transmitter locations. Their legends also show the antenna height (h) above ground level for each transmitter.

A. Measurement scenario and setup

Mining complex 1, Figure 1, has been in exploration since 1942 and comprises an area of approximately 60 km^2 (12 km $\times$ 5 km), with three main pits. The altitude of the highest transmitter, is 1300 meters above the sea level, while the lowest receiver position is located at an altitude of 810 meters. Anticipating the deployment of heterogeneous networks (HetNet), small cells have been incorporated, at this layer the absolute altitude difference is limited to 300 meters. Mine 2, Figure 2, a single-pit mine inaugurated in 2006 has an area of approximately 9.2 km^2 (4 km $\times$ 2.3 km). The altitude variation between transmitters and receiver positions in this mine ranges from 400 meters at the macro layer to 200 meters at the small cell layer.

Since open-pit mine terrain characteristics differ from those found in urban and suburban scenarios, it is important to redefine terms as macro and small cells. As done in [11], we define a small cell deployment as the one where the transmitter is placed closer to the ground level, below the median altitude of the covered area. A macro cell deployment, on the other hand, is defined as the one in which the transmitter is placed in an elevated position, above the median altitude of the covered area. The location of macro and small cells was chosen based on the available infrastructure (radio towers, cell-on-wheels (COW), power sources), accessibility, safety and also relevance to network coverage. Prior to the measurement campaign, a preliminary network coverage planning was done with a commercial software, to support the transmitters placement and ensure that relevant areas would be covered.

The measurements are taken in the 2.6 GHz and 700 MHz bands due to their importance to the mining industry. First, both of these bands are in the operational bands of LTE systems, which is a promising technology candidate for mission-critical communications [12]. Second, the usage of part of the 700 MHz spectrum band is under discussion in Brazil to support infrastructure and mission critical communications. Third, the 2.6 GHz band is also close to the 2.4 GHz ISM band, which is widely used in wireless networks deployments in open-pit mines in Brazil, and around the world [1]. Besides these three reasons, sub-6 GHz frequencies are already envisioned as a fundamental part of upcoming 5G technologies, specially in earlier implementation phases [7].

Two continuous wave (CW) signals were generated by a couple of Agilent signal generators (models E4438C and E4421B), combined, and transmitted on a single dual-band omni-directional antenna, with 60° elevation beamwidth. The transmitter antenna gain is 4 dBi for the 700 MHz band, and 6 dBi for the 2.6 GHz band. In all transmitters at the 700 MHz band, the EIRP was approximately 20 dBm. Small cell deployments in 2.6 GHz band EIRP was approximately 17 dBm. At the 2.6 GHz band macro cell deployments, the signal was amplified before combining in order to extend the measurement range. The final EIRP was around 50 dBm.

The receiver was mounted on a vehicle rooftop, at 1.8 m height, with two dual-band omni-directional antennas of gain equal to 1.1 dBi. The vehicle was driven at an average speed of 35 km/h and all the routes were repeated at least twice. The received signal strengths and GPS locations were collected simultaneously at both frequencies, using an R&S TSMW Universal Radio Network Analyzer at a rate of 150 samples/s.

B. Data Processing

From the measurements, the path loss per link (L) can be estimated by:

$$L = P_{TX} + G_{TX}(\theta) + G_{RX} - P_{RX} - L_{\mathrm{c}} \quad (1)$$

where P_{TX} represents the transmitted power, in dBm, P_{RX} represents the local mean received power, also in dBm, averaged over 40λ of the 700 MHz band signal in order to remove the fast fading [14], [16], L_{c} represents the combined cable losses, in dB, at both Tx and Rx sides, $G_{TX}(\theta)$ and G_{RX} are the Tx and Rx antenna gains, in dB, respectively. It is important to mention that we have compensated the antenna pattern according to the elevation angle, θ, in degrees, between transmitter and receiver.

The analysis proceeds with the parametrization of a statistical large-scale path loss model. In this work, we chose to parametrize the alpha-beta (AB) model with floating intercept [17], in order to highlight the differences between the considered scenarios. Those differences will be further discussed in Section III. The interested reader can find the mathematical formulation of the AB model in the Appendix.

By removing the estimated mean path loss over segments of 50 meters, l_n, we create a local mean fading process representing the random variations on the local mean. Assuming that the path loss model in Eq. 6 (Appendix) is able to predict the local mean, this random process corresponds to the shadow fading term that is usually considered in the multiplicative fading model [16]. The shadowing standard deviation can be calculated as:

$$\sigma_{SF} = \sqrt{\frac{\sum_{n=1}^{N} (L_n - l_n)^2}{N-1}} \quad (2)$$

where L_n represents n^{th} measured path-loss sample. Although there is no direct link between the predictions from Eq. 1 and the local mean, it is still useful to characterize the correlation properties of the local mean fading process.

From the shadowing samples, $X_n = L_n - l_n$, we can also estimate the sample autocorrelation, $R_{XX}(d_k)$, as a function of discrete distances, d_k, as [13]:

$$R_{XX}(d_k) = \frac{\sum_{n=1}^{N-k} X_n X_{n+k}}{\sum_{n=1}^{N} X_n^2} \quad (3)$$

where X_n represents the shadow fading at n^{th} distance, and $d_k = k\Delta d$. In order to calculate, we have quantized the distances, d_k, with $\Delta d = 1$ meter.

Until now, all the processing was done considering one frequency at a time. However, since the measurements on both frequencies were taken simultaneously, and over the same routes, we can also calculate the inter-frequency shadowing correlation coefficient, ρ_{xy}:

$$\rho_{xy} = \frac{\sum_{n=1}^{N} X_n Y_n}{\sqrt{\sum_{n=1}^{N} X_n^2 \sum_{n=1}^{N} Y_n^2}} \quad (4)$$

where X represents the shadowing at the 700 MHz band, and Y denotes the shadowing at the 2.6 GHz band.

III. Results and Discussion

In this section we discuss the results from the measurement campaign, presented in Table I. Path loss models are given in terms of the path loss exponent, α, the intercept, β, and root-mean-square error (RMSE). Table I also shows the values of shadowing standard deviation, σ_{SF}, autocorrelation distances, d_{corr} and inter-frequency shadowing correlation. The results are summarized in Table I. Differences in the topography in mines 1 and 2 led to distinct path loss models for macro cell deployments. Mine 1 has at least three pits in an inverted-pyramid shape, where the measurements were located. Mine 2, on the other hand, is a hillside mine with no pits as deep as those in Mine 1. The same difference was not observed in the models for small cells. Therefore, we present two macro cell models, one for mine 1, and one for mine 2, and a single small cell model.

A. Path Loss Models

Path loss measurements and models for macro cell transmitters in mine 1 are shown in Figure 3, considering both the 700 MHz band, in blue, and the 2.6 GHz band, in red. The path loss exponents are 2.3 and 2.1 respectively, and the intercept points are 36 and 62.7 dB. As in [11], we do not distinguish between LOS and NLOS propagation, because there is no clear breakpoint distance in case of macro cells in open-pit mines. The RMSE in each case is 10.7 and 12 dB. Results for the macro cells in Mine 2 are shown in Figure 4, considering the two studied spectrum bands. Once again, similar path loss exponents were found for both frequencies: 3 and 2.8 for the 700 MHz and 2.6 GHz band respectively, ant β values are 8.9 and 29.8 in each case. The RMSE in each case is 10.7 and 12.4 dB.

Table I
Summary of Large-scale propagation parameters

	Macro Cell				**Small Cell**	
	Mine 1		**Mine 2**		**All**	
f [GHz]	0.7	2.6	0.7	2.6	0.7	2.6
α_{LOS}	2.3	2.1	3.0	2.8	2.4	2.5
α_{NLOS}					3.7	3.7
β_{LOS}	36	62.7	8.9	29.8	30	38.5
β_{NLOS}					4.9	15.9
$RMSE_{LOS}$	10.7	12	10.7	12.4	7	6
$RMSE_{NLOS}$					8.7	7.9
$\sigma_{SF_{LOS}}$	10	12.3	9.5	11	8.4	7.5
$\sigma_{SF_{NLOS}}$					7.5	7.2
$d_{corr,LOS}$	78.6	80.3	68.5	63.5	19.3	16.6
$d_{corr,NLOS}$					15	13.7
ρ_{xy}	0.87		0.92		0.81	

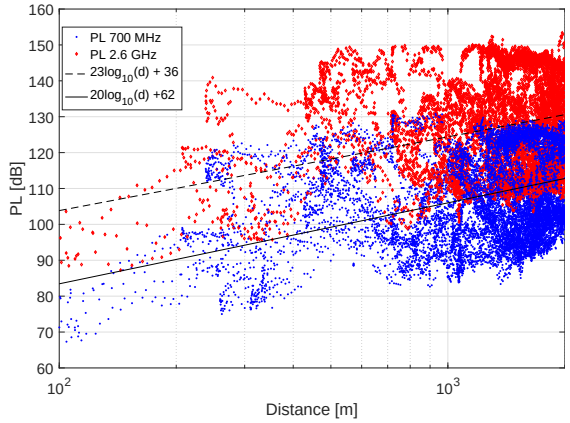

Figure 3. Path loss and linear regression for macro cell deployments in mine 1, at 2.6 GHz and 700 MHz band. Shadow fading standard deviation, σ_{SF}, equals 10 dB and 12.3 dB for the 700 MHz and 2.6 GHz bands respectively.

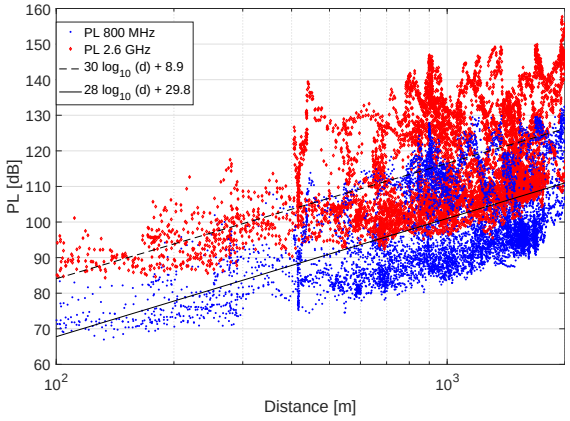

Figure 4. Path loss and linear regression for the macro cell deployments in mine 2, at 2.6 GHz and 700 MHz band. Shadow fading standard deviation, σ_{SF}, equals 9.5 dB and 11 dB for the 700 MHz and 2.6 GHz bands respectively.

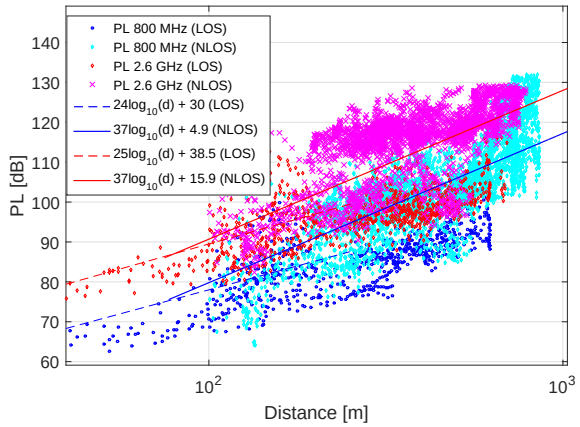

Figure 5. Path loss and linear regression for the small cells in mines 1 and 2, at 2.6 GHz and 700 MHz band. LOS Shadow fading standard deviation, $\sigma_{SF_{LOS}}$, equals 8.4 dB and 7.5 dB for the 700 MHz and 2.6 GHz bands respectively. $\sigma_{SF_{NLOS}}$ equals 7.5 and 7.2 dB.

The results of small cells are aggregated in Figure 5. In the case of small cells, there is a clear breakpoint distance between LOS and NLOS data. We present the path loss model based on the LOS conditions, and the brekpoint distance is defined where the LOS model intersects the NLOS model. For the LOS part, the path loss exponent is 2.3 for both frequencies, close to the free space path loss exponent, where α equals 2. This is aligned with the literature for small cells in urban deployments [15], [18]. The frequency dependent offset between the path loss in each frequency is 8.5 dB, compared to the 10.2 dB expected from the free space path loss difference. Considering the NLOS measurements, we found path loss exponents of 3.7 considering both the 700 MHz and the 2.6 GHz band.

B. Shadowing

Shadowing standard deviations, σ_{SF}, (Table I) are similar at both frequencies in most deployments. The shadowing standard deviations in macro cells are between 9.5 and 12.3 dB, and in small cells they are in the range of 7.2 and 8.4, depending of the line-of-sight conditions. Macro cell shadowing values are slightly higher than those recommended for the evaluation of urban macro and rural macro scenarios [19], which are 8 dB in NLOS conditions. These values will significantly impact the design of ultra-reliable networks in open-pit mines, since larger values of σ_{SF} imply larger shadow fading margins in order to obtain a certain network availability.

C. Shadowing correlation distance

Besides the standard deviation of σ_{SF}, it is important to also investigate the spatial autocorrelation of the shadowing process, relevant to the parametrization of handover procedures. The correlation distance is calculated as the distance where the autocorrelation, Eq. 3, reaches the value of $1/e$, and usually modeled as a first-order autoregressive process, implying an exponential decay [21]. For each transmitter, we calculated the autocorrelation considering contiguous drive-test routes of 1 km for macro cells, and 150 meters for small cells. We tested different route lengths and observed that the autocorrelation value does not change significantly for routes longer than 1 km in macro cell deployments. Small cell route lengths were chosen for the LOS and NLOS characteristics. In each case, we calculated the autocorrelation using lags within one third of the route distance. The final results are calculated as an average of each of the autocorrelation in each one of those routes. The results for three macro cell deployments in 700 MHz and 2.6 GHz bands are shown in Figure 6 and detailed in Table I. Similar results were obtained for other macro and small cell deployments, but omitted from the figure due to lack of space.

Average correlation distances for macro cells deployed in mine 1 are 78.6 and 80.3 meters at 700 MHz and 2.6 GHz bands, respectively. For macro cells deployed in mine 2, these values are lower: 68.5 and 63.5 meters. These values fall within the range between urban deployments, 50 meters, and rural deployments, 120 meters [19]. These results are justified by considering that the mine topography is more rugged than a

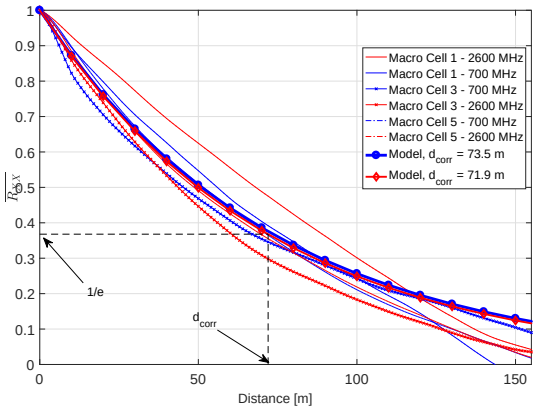

Figure 6. Shadow fading autocorrelation at both frequency bands, considering the deployments at mines 1 and 2

rural area, but there are not as many obstructions, such as buildings, as in a urban scenario. The model presented in [21] with the average values in each frequency band, 73.5 m and 71.9 m, is also shown in Figure 6.

Considering small cells in LOS, average correlation distances are 19.3 and 16.6 meters, at 700 MHz and 2.6 GHz respectively. In NLOS conditions, these values are 15 and 13.7 meters. These values are slightly higher than those recommended for urban micro deployments in [19], which are respectively 10 and 13 meters.

D. Inter-frequency shadowing correlation

Finally, we investigate the inter-frequency shadow fading correlation ρ_{xy} in the 700 and 2600 MHz frequency bands. The shadow fading correlation is an important measure of the advantages of using inter-frequency multi-connectivity as a technique to enhance the availability of wireless systems, as presented in [22].

The results are shown in Table I. The macro cell results show values between 0.87 and 0.92, while small cell results show ρ_{xy} equal to 0.81. Highly correlated shadowing processes are expected at similar frequency bands, for example 1 or 2 GHz apart, since both experience the same shadowing effects. The results at the mine environment are in agreement with those observed in urban deployments, at the 955 MHz and 1.8 GHz bands [15].

E. Discussion

Knowledge about large-scale propagation is fundamental in the design and performance evaluation of wireless networks, especially when considering the strict availability requirements of URC networks. Here, we discuss the results in light of the impact they will have on the design of wireless networks in open-pit mines.

Path loss exponents and intercept values, for example, are very useful for quick link budget and system capacity estimation. The results show that, similar to urban deployments [15], the path loss exponents are comparable in the two frequency bands. Differences in the mines topographies led to distinct path loss models. In the first mine, path loss exponents in the order of 2 were found, and in the second mine, those exponents were in the order of 3. Considering small cells, the results are shown according to the LOS conditions. In the LOS part, exponents in the order of 2, and in the NLOS part, they are in the order of 4. Differences between macro and small layers can also be exploited on the design of ultra-reliable heterogeneous wireless networks in open-pit mines. For example, in co-channel deployments, high path loss exponents provide a natural isolation from interference [3].

Shadowing standard deviations for macro cells, are between 9.5 and 12.3 dB considering both frequency bands. For small cells, the shadowing standard deviation is between 7.2 and 8.4 depending on the frequency and LOS conditions. Macro cell values are slightly higher than those found in urban, suburban and industrial environments. The direct implication is the increase in shadow fading margins in order to support URC, leading to denser networks. For example, considering a log-normal shadowing, the availability (probability that the received signal power x is higher than a threshold x^{URC}) is calculated as [20]:

$$P(x > x^{URC}) = 1 - Q\left(\frac{SF_{margin}}{\sigma_{SF}}\right) \quad (5)$$

where Q is the error function: $Q(x) = \frac{1}{2}\text{erfc}\left(\frac{x}{\sqrt{2}}\right)$. An outage probability in the order of 10^{-5} considering the most restrictive σ_{SF} for macro cells, 12.3 dB, as a simple consideration, would require a shadow fading margin of 50 dB. For small cells, considering the highest σ_{SF} value, the necessary margin would be 35 dB. Considering the same outage probability, indoor industrial environments need, in contrast, a shadow fading margin of 28 dB according to [20].

Shadowing correlation distances were similar for macro cells in both frequency bands: approximately 72 meters. Considering small cells, the LOS correlation distance is between 16.6 and 19.3 meters, and the NLOS correlation distance is between 13.7 and 15 meters. These values are higher than those found in urban deployments, and smaller than the recommended for rural environments, and should be considered in the parametrization of handover procedures in open-pit mines. Parameters like time-to-trigger and hysteresis need to be set accordingly based on the scenario and cell-type, in order to balance the probability of handover and the probability of outage. Furthermore, the speed of the user-equipment (UE) need to be considered. In the mine, this is quite diverse: while as drillers and bulldozers are most of the time static or subject to very limited mobility, hauling trucks can drive up to 50 km/h within the main mine routes.

Finally, we presented the inter-frequency cross-correlation of shadowing for deployments at 700 MHz and 2.6 GHz. The correlation values are between 0.81 and 0.92 in macro and small cell deployments. In [22], the author investigates the availability gains when using simultaneously different carrier frequencies to send data through the network. Different com-

binations of frequencies were investigated, in the sub-6 GHz band (2 and 2.5 GHz) and in also in the mmWave spectrum (15, 28 and 73 GHz). In all cases, as the shadowing correlation between the frequencies increases, the availability gain obtained through multi-connectivity reduces, for there is no diversity with respect to shadowing. However, it is important to highlight that the network can still exploit path diversity. Following the same analysis presented in [22], our results indicate that the availability gain of multi-connectivity in this combination of frequencies, 700 MHz and 2.6 GHz bands, can be rather limited in open-pit mines.

IV. Conclusion

In this paper, we presented original results from an extensive measurement campaign in a industrial setting where sub-6GHz 5G wireless systems are expected to play an important role in the near future, namely open-pit mines. We have focused on large scale propagation at the 700 MHz and 2.6 GHz frequency bands. The results show that mine topography significantly impact the macro cell path loss models. Furthermore, shadow fading statistics (standard deviation, autocorrelation distances, inter-frequency shadowing correlation) have been diligently examined for both bands in HetNet scenarios. Observed shadow fading variances of up to 12.3 dB will imply network densification in order to achieve URC availability requirements. Furthermore, we have observed high inter-frequency shadowing correlation, which limits the availability gains of multi-connectivity in this combination of frequencies. Our results will be useful for the design, modeling and evaluation of wireless networks supporting unmanned mining initiatives.

Appendix A
AB model

The AB model consists in a linear regression of the L_{dB} estimates considering a floating intercept. The path loss ($PL_{[dB]}$) is modeled as:

$$PL(d)_{[dB]} = \alpha \cdot 10\log_{10}(d_{[m]}) + \beta \tag{6}$$

The path loss exponent α and the floating intercept β can be obtained by a least square linear regression of the path loss, L, estimates obtained in Eq. 1:

$$\alpha = \frac{\sum_{n=1}^{N}(D_n - \overline{D})(L_n - \overline{L})}{\sum_{n=1}^{N}(D_n - \overline{D})^2} \tag{7}$$

$$\beta = \overline{L} - \alpha \times \overline{D} \tag{8}$$

where $D_n = 10\log_{10}(d_{n_{[m]}})$ is the 3D distance, in logarithmic scale, between the transmitter and the n^{th} average distance range, and $\overline{D}$ represents the average distance, also in logarithmic scale, over the considered data set. L_n represents the path loss estimate at the n^{th} average point, and $\overline{L}$ represents the average path loss over the considered data set. We also consider the root mean square error $RMSE = \sqrt{\frac{\sum_{n=1}^{N}(L_n - PL_n)^2}{N}}$.

Acknowledgment

The authors would like to thank the Operational Techonlogy and Information Technology teams from Vale S.A. for their valuable inputs and help during the measurement campaign.

References

[1] S. Vellingiri et al. "Energy efficient wireless infrastructure solution for open pit mine." *Advances in Computing, Communications and Informatics (ICACCI)*, 2013, 1463-1467.

[2] T. Sens, *Private LTE a game changer for industries*. Available on: https://blog.networks.nokia.com/lte/2016/04/21/private-lte-game-changer-industries/. Accessed on July, 2017.

[3] L. G. U. Garcia et al. "Mission-critical mobile broadband communications in open-pit mines." *IEEE Communications Magazine 54.4* (2016): 62-69.

[4] V. S. B. Barbosa et al. "The Challenge of Wireless Connectivity to Support Intelligent Mines." *24th World Mining Conference (WMC)*, 2016.

[5] A. Boulter, et al. "Wireless network requirements for the successful implementation of automation and other innovative technologies in open-pit mining." *International Journal of Mining, Reclamation and Environment.* (2015): 368-379.

[6] A. Frotzscher et al., "Requirements and current solutions of wireless communication in industrial automation", *Communications Workshops (ICC), 2014 IEEE International Conference on.*, June 2014.

[7] ITU,"IMT vision - Framework and overall objectives of the future development of IMT for 2020 and beyond", Rec. ITU-R M.2083-0, Sep. 2015.

[8] A. E. Forooshani et al. "A survey of wireless communications and propagation modeling in underground mines." *Communications Surveys & Tutorials, IEEE 15.4 (2013):* 1524-1545.

[9] J. J Aitken, "Development of a radio propagation model for an open cut mine", *20th International Electronics convention & exhibition*, 1985.

[10] R. Nilsson, et al. "Channel Measurements in an Open-pit Mine using USRPs: 5G–Expect the Unexpected." *Wireless Communications and Networking Conference (WCNC)*, 2016.

[11] E. P. L. Almeida et al. "Radio Propagation in Open-pit mines: a first look at measurements in the 2.6 GHz Band." *28th Annual IEEE International Symposium on Personal, Indoor and Mobile Radio Communications, (PIMRC), 2017.*

[12] GSMA. *Network 2020: Mission Critical Communications*. GSMA, 2017.

[13] E. Tanghe, et al. "The industrial indoor channel: large-scale and temporal fading at 900, 2400, and 5200 MHz." *IEEE Transactions on Wireless Communications 7.7* (2008).

[14] N. S. Adawi et al, "Coverage Prediction for mobile radio systems operating in the 800/900 MHz frequency-range." *IEEE Vehicular technology society committee on radio propagation. IEEE Transactions on vehicular technology 37.1* (1988).

[15] P. Mogensen et al. "Urban area radio propagation measurements at 955 and 1845 MHz for small and micro cells." *Global Telecommunications Conference, 1991. GLOBECOM'91.'Countdown to the New Millennium. Featuring a Mini-Theme on: Personal Communications Services.* IEEE, 1991.

[16] W. C. Y. Lee, *Mobile Communications Engineering*, 2nd Edition, McGraw Hill, 1983.

[17] S. Sun, et al. "Investigation of prediction accuracy, sensitivity, and parameter stability of large-scale propagation path loss models for 5G wireless communications." *IEEE Transactions on Vehicular Technology 65.5* (2016): 2843-2860.

[18] I. Rodriguez, *An Empirical Study on Radio Propagation in Heterogeneous Networks: with Focus on Mobile Broadband Networks and Small Cell Deployment*. Diss. Aalborg Universitetsforlag, 2016.

[19] M. Series, *Guidelines for evaluation of radio interface technologies for IMT-Advanced.* Report ITU 2135-1 (2009).

[20] B. Singh et al. "Ultra-reliable communication in a factory environment for 5G wireless networks: link level and deployment study." *Personal, Indoor, and Mobile Radio Communications (PIMRC), 2016 IEEE 27th Annual International Symposium on.*IEEE, 2016.

[21] M. Gudmundson, "Correlation model for shadow fading in mobile radio systems." *Electronics letters 27.23* (1991): 2145-2146.

[22] D. Öhmann, et al. "Achieving high availability in wireless networks by inter-frequency multi-connectivity." *Communications (ICC), 2016 IEEE International Conference on.* IEEE, 2016.